

High-pressure transport and microcalorimetry studies on high quality YbCu₂Si₂ single crystals

E. Colombier, D. Braithwaite, G. Lapertot, B. Salce, and G. Knebel
 INAC/SPSMS/IMAPEC, CEA-Grenoble, 17 rue des Martyrs, 38054 Grenoble Cedex 9, France
 (Received 20 June 2008; published 11 June 2009)

We report electrical transport and calorimetry studies on high quality single crystals of YbCu₂Si₂ under pressure in diamond and Bridgman anvil pressure cells with liquid pressure-transmitting media. At ambient pressure, in the best samples we find residual resistivities of less than 0.5 $\mu\Omega$ cm. We have also determined the anisotropy of the temperature dependence of the resistivity and shown that this can account for sample-dependent differences of the resistivity. We confirm the previously reported transition to a magnetically ordered ground state with pressure and we have precisely determined the (p, T) phase diagram using pure samples, good hydrostatic pressure conditions, and calorimetry measurements. Above 8.8 GPa we see a clear signature of the transition in the specific heat. We discuss the low-temperature resistivity and specific-heat behaviors in respect to the universal Kadowaki Woods ratio, to other ytterbium-based strongly correlated systems, and to the cerium-based counterpart, CeCu₂Si₂.

DOI: [10.1103/PhysRevB.79.245113](https://doi.org/10.1103/PhysRevB.79.245113)

PACS number(s): 71.27.+a

I. INTRODUCTION

One of the major motivations for the study of heavy fermion systems is that a quantum phase transition between magnetic and nonmagnetic ground states can be relatively easily attained by applying pressure to tune the competing Kondo and Ruderman-Kittel-Kasuya-Yoshida (RKKY) interactions. Many studies on cerium-based systems now show that when a magnetic quantum critical point (QCP) is approached in this way, several other phenomena are found, including deviations from Fermi-liquid theory in the electronic terms of resistivity and specific heat, and most spectacularly, unconventional superconductivity.¹ Yb is often considered to be the “hole” equivalent of cerium. Pressure tends to drive Yb from its nonmagnetic Yb²⁺ ($4f^{14}$) state to a magnetic Yb³⁺ ($4f^{13}$) state and so similar phenomena to those found in cerium systems might be expected. However there are, to date, far fewer studies on Yb-based compounds. This is partly for practical reasons. Preparing very pure single crystals of the ytterbium-based systems has often proved difficult and higher pressures are usually necessary. In most of the cerium compounds studied, a pressure of 2–3 GPa is sufficient to attain the QCP and this can be easily achieved in standard clamp pressure cells with relatively good hydrostaticity. The ytterbium systems often require pressures of 8–10 GPa. Nevertheless, differences are starting to emerge between the QCPs of the two families and so far superconductivity close to a critical point has only been found in one ytterbium-based system.² Understanding these differences is an essential step and is the motivation for a new generation of experiments on pure crystals and in good hydrostatic conditions and YbCu₂Si₂ is an ideal case for this. Previous studies showed that at ambient pressure it is in an intermediate-valence state and that a magnetic transition is induced for pressures above 8 GPa.^{3–5} These studies were performed on polycrystals with residual resistivities of several $\mu\Omega$ cm and in quasihydrostatic conditions. We report here on the growth of a new batch of very high-purity single crystals. We have characterized them by measurements of their anisotropic resistivity and specific heat at ambient pres-

sure. Then we have performed resistivity and ac calorimetry experiments under pressure in hydrostatic conditions using diamond-anvil cells with argon as pressure-transmitting medium or a newly developed modified Bridgman cell with liquid (fluorinert) pressure-transmitting medium. The aim of this study is to define more precisely the magnetic phase diagram using the ac calorimetry technique, notably to follow the magnetic transition to lower temperatures and determine if possible whether a second-order QCP exists, to measure the low-temperature behaviors of the resistivity and specific heat under pressure and to measure resistivity at very low temperature close to the QCP in order to search for a possible occurrence of superconductivity.

II. EXPERIMENTAL DETAILS

Single crystals of YbCu₂Si₂ were grown by an indium flux method. Ytterbium, copper, and silicon in stoichiometric amounts were put together with excess indium in a MgO crucible. The crucible was sealed in a quartz tube and heated to 850 °C for one week. Annealing of the samples was then performed for two weeks at 850 °C with a slow decrease in ambient temperature. We also prepared in the same way crystals YbCu₂Si₂ with an Al₂O₃ crucible. We obtained plate-shaped crystals (1–2 mm² and a few hundred micrometers thick). A Laue x-ray diffractometer was used to orientate some crystals and showed that the large surface of the platelets corresponds to the a - b plane. These crystals were either polished to a thickness of about 40 μ m and then cleaved into small pieces for measurements under pressure, or cut into bar-shaped pieces using a diamond or wire saw for ambient pressure measurements. Samples were characterized at ambient pressure by resistivity and specific-heat measurements. Resistivity was measured by a conventional four-point technique down to 0.5 K in a commercial device [Quantum Design Physical Property Measurement System (PPMS)] and in a few cases in a dilution refrigerator down to about 60 mK. The specific heat at ambient pressure was also measured in the PPMS. Resistivity measurements under pressure were performed using diamond-anvil cells with 1

mm culets up to 7.55 GPa and in modified Bridgman cells⁶ with a liquid medium (fluorinert) up to 7.8 GPa. The Bridgman cells were measured in the PPMS between 300 and 2 K and in some cases were also measured in the dilution fridge down to 60 mK. The diamond-anvil cells were measured in the ³He cryostat up to 4.5 GPa and in the ⁴He cryostat up to 7.5 GPa. We also measured specific heat by ac calorimetry⁷ in a diamond-anvil cell with 0.7 mm diamond culet flats. An Au:Fe (0.07%) thermocouple was spot welded on the sample to ensure a good thermal contact. The sample was heated by an alternative excitation provided by a regulated laser diode and brought against the diamond window through an optical fiber. Measurements were performed at a frequency of 1900 Hz which, from the signal-frequency dependence, was found to be high enough to thermally separate the sample from its environment. A treatment using a measurement at low frequency (17 Hz) confirmed 1900 Hz to be a suitable frequency and that the influence of the thermal link to the bath could be neglected. From the thermocouple voltage measured and the thermoelectric power of the thermocouple we obtained the value of the temperature oscillations which is inversely proportional to the specific heat. Measurements were performed between 10 and 1.4 K up to 11 GPa in the ⁴He cryostat with the *in situ* pressure-tuning device.⁸ Attempts were also made to measure at fixed pressures down to 500 mK in the ³He cryostat or to lower temperatures in the dilution refrigerator, though we later found that the data below 500 mK was not reliable as too much power had been applied. Typical values of the amplitude of the temperature oscillations T_{ac} of the sample were 1.5 and 0.5 mK at 0.5 and 1.3 K, respectively. The average warming T_{dc} of the sample compared to the bath was estimated to be around 10 and 2 mK, respectively.

For all measurements in the diamond cells, argon was used as a pressure medium. In the ⁴He cryostat the pressure could be changed *in situ*⁸ allowing higher pressures to be reached but the lowest temperature was about 1.5 K. Ruby chips were placed inside the pressure chamber to determine the pressure over the whole temperature range from the ruby fluorescence. In the modified Bridgman cell, the superconducting transition temperature of a lead manometer was used to determine pressure at low temperature.

III. RESULTS AND DISCUSSION

A. Resistivity anisotropy and specific heat at ambient pressure

The residual resistivity ratio (RRR) is a good test of sample quality. In previous studies on YbCu₂Si₂ an RRR of 20 between 1.2 and 300 K was reported on polycrystalline samples⁴ and RRR=40 between 2 and 300 K was found on single crystals.⁹ In our study in order to perform fast characterizations on many samples, the resistivity was measured only down to 1.8 K so we took as the criterion the ratio between the values at 300 and 2 K, $RRR_{2-300\text{ K}}$. The resistivity ratio of the samples grown in an Al₂O₃ crucible was around 20 even after annealing. On the other hand the single crystals grown in a MgO crucible had typical resistivity ratios $RRR_{2-300\text{ K}}$ between 90 and 120, which is a remarkable improvement on all previous reports and corresponds to re-

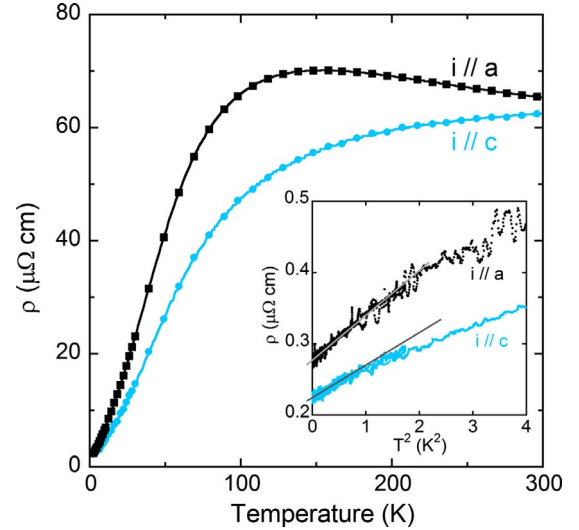


FIG. 1. (Color online) Temperature dependence of the resistivity tensor components deduced from a sample in the Montgomery configuration. Inset: low temperature linear dependency of ρ versus T^2 from measurements on bar-shaped samples

sidual resistivity values of less than 0.5 $\mu\Omega$ cm. In the following we will show only samples grown in MgO crucibles. We observed large differences in the high-temperature part of the curves between samples. For most samples the resistivity increases when T decreases from 300 to around 200 K, and a maximum in the resistivity exists. Most samples with resistivity curves presenting a clear resistivity maximum have very good resistivity ratios. This maximum was not observed in earlier studies on polycrystals, however a maximum in the resistivity was previously found under pressure and was found to be sample dependent. This sample dependence was tentatively ascribed to anisotropy⁵ which was suspected as quite strong anisotropy in the magnetic susceptibility at ambient pressure was already reported.^{10,11}

To check this, we used the Montgomery method¹² to determine the resistivity tensor components. Two oriented samples were cut into rectangular-shaped samples with dimensions of about $400 \times 300 \mu\text{m}$ in the (a, c) plane with a thickness of 100 μm . Both samples gave similar results (Fig. 1) for resistivity along a axis and c axis. We observe an increase in the resistivity ρ_a when T decreases from 300 to 170 K and a continuous decrease in ρ_c . This confirms that although the resistivity is almost isotropic at 300 K, the temperature dependence is strongly anisotropic and can probably explain the sample dependent differences that are observed.

A disappointing point of this Montgomery sample is the low-resistivity ratio $RRR_{2-300\text{ K}}$ compared to our other samples, lower than 30 for both orientations. Furthermore in the Montgomery configuration, the signal measured at low temperature was very small and did not allow an accurate determination of the dependence of the resistivity at low temperature. We then measured two thin samples bars oriented along the a axis and the c axis, respectively, with typical dimensions 300 μm long and $100 \times 100 \mu\text{m}^2$ cross section down to 60 mK in a dilution fridge. We obtained for both samples excellent resistivity ratios and the high-temperature curve was very similar to the Montgomery

method results. For ρ_a , we found a resistivity ratio of 167 between 300 and 2 K and 208 for ρ_c . These bar-shaped samples allowed a precise determination of the low-temperature resistivity behavior. In previous reports, whereas a Fermi-liquid behavior was found in specific-heat measurements,^{9,11} it was not so clear for resistivity measurements. Alami-Yadri *et al.*^{3,4} report a T^2 dependence below 4 K (and $T^{1.3}$ for $1.2 < T < 10$ K) while Tsujii *et al.*⁹ found no T^2 dependence but a $T^{1.4}$ between 1.8 and 20 K with a single crystal made by a similar indium flux method. From our measurement, we find T^2 dependence from 60 mK up to 0.9 K for ρ_c and up to 1.4 K for ρ_a . The A coefficient from the T^2 fit is $0.071 \mu\Omega \text{ cm/K}^2$ along the a axis, similar to that found in previous studies,³⁻⁵ and $0.044 \mu\Omega \text{ cm/K}^2$ along the c axis. From this low-temperature T^2 fit, we obtain $\rho_0 = 0.27 \mu\Omega \text{ cm}$ along the a axis and $\rho_0 = 0.22 \mu\Omega \text{ cm}$ along the c axis and we obtain the residual resistivity ratio $\text{RRR}_{0-300 \text{ K}} = 295$ and 332, respectively. We deduce that there is no strong anisotropy of ρ_0 or of the residual resistivity ratio.

We performed specific-heat measurements down to 1 K and we found a C/T linear dependence versus T^2 with $\gamma = 155 \text{ mJ/Mol K}^2$. Two previous specific-heat measurements found $\gamma = 135 \text{ mJ/mol K}^2$ (Ref. 11) and $\gamma = 150 \text{ mJ/mol K}^2$ (Ref. 9) from a fit $C/T = \gamma + \beta T^2$ with $T < 10$ K. This latter value is close to ours. We observed a maximum in C/T for $T = 72$ K which is attributed to crystal-field effects and compatible with the maximum in the resistivity.

B. ac calorimetry and resistivity under pressure

First we show the measurements in the ^4He cryostat. Figure 2(a) shows the low-temperature measurements obtained for pressures below the transition appearance ($p < 8.3$ GPa). In order to compare measurements in different conditions, the data were normalized at 6 K. Above 5 K all the curves scale well but below 5 K and above 3 GPa, an upturn of C/T occurs and becomes more pronounced with increasing pressure.

Figure 2(b) compares the normalized specific heat over temperature for pressures of 8.8 GPa and above where we observed a distinctive anomaly corresponding to the magnetic transition. The criterion we took to determine the transition temperature is defined as shown in the inset of Fig. 2(b), however if a different criterion, for example, the inflection point of the increase or the maximum of C/T is taken, the resulting ordering temperature is not changed by more than about 0.15 K. The divergence of C/T on approaching the transition is qualitatively in agreement with the behavior expected from spin-fluctuation theory¹³ and the curves are qualitatively quite similar to those for example of $\text{CeCu}_{6-x}\text{Au}_x$ near its critical point.¹⁴

In order to detect the appearance of the magnetic phase at lower pressures, attempts were made to measure at low temperature, in ^3He and dilution cryostats, at a few fixed pressures as shown in Fig. 2(c). The results are not conclusive, at 8.1 GPa the C/T curve is, for some unknown reason, quite different from the ones obtained at similar pressures in the

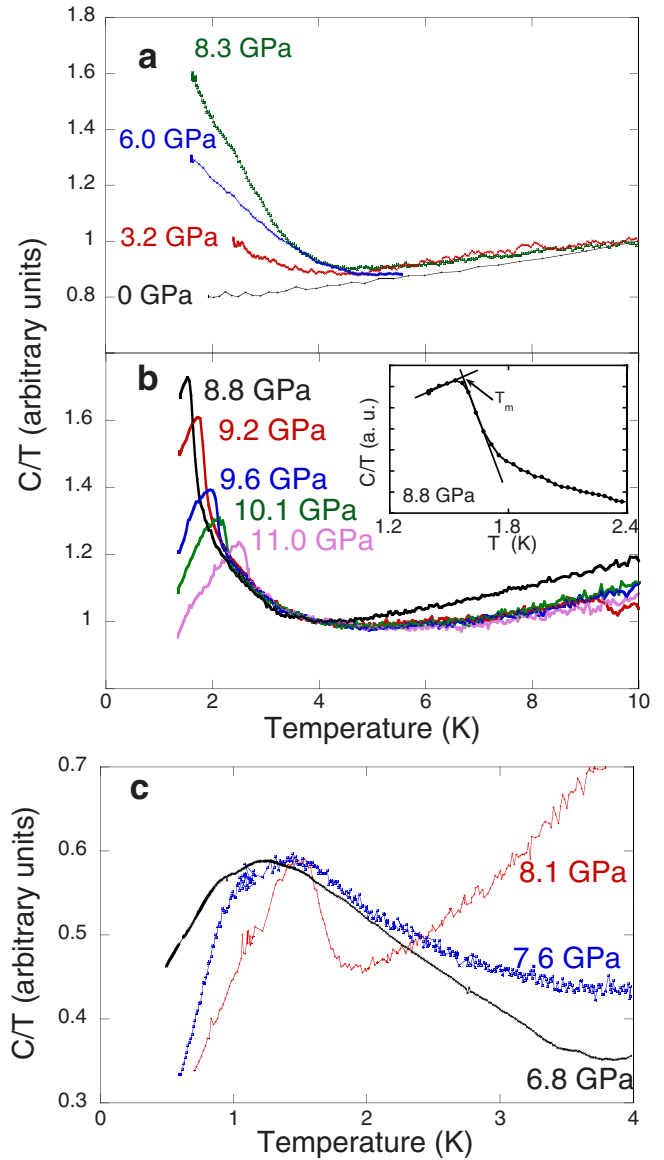


FIG. 2. (Color online) Specific heat versus temperature by ac calorimetry. For comparison, data were normalized at the high temperature (6 K). Figure 2(a) (top) shows curves for pressures below the critical pressure up to 8 GPa. Figure 2(b) (middle) shows normalized curves for pressures above 8.8 GPa. The inset shows the criterion used to determine the transition temperature. Figure 2(c) shows measurements at lower temperatures close to the critical pressure (please note different temperature scale). A clear transition appears at 8.1 GPa but at lower pressures only a broad pressure-independent feature is seen.

other experiments, however a clear, sharp transition seems to be present at about 1.6 K. At lower pressures the transition changes to a broad maximum and centered at about 1.5 K, which seems rather insensitive to pressure and which may or may not be related to the appearance of magnetic order.

Figure 3 summarizes the transition temperatures obtained by ac calorimetry under pressure. The point obtained from resistivity around 7.8 GPa is also plotted (see later discussion), as well as the data from previous resistivity studies.^{4,5} The solid line indicates the well-defined transition points.

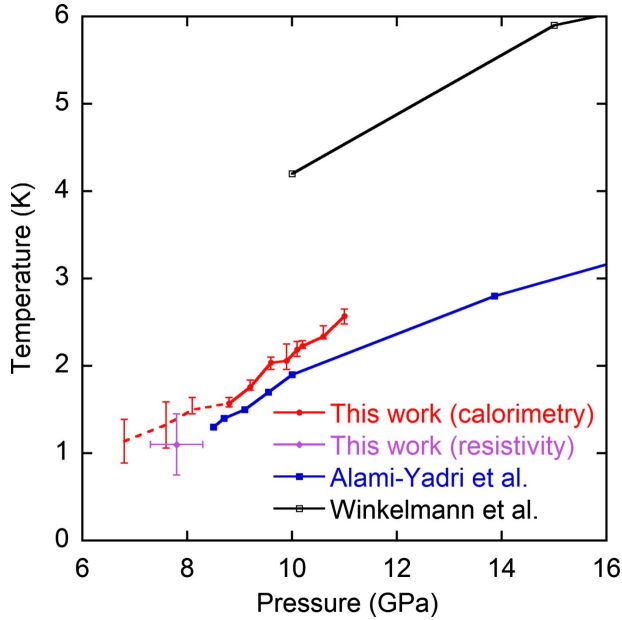


FIG. 3. (Color online) Transition temperature dependence with pressure from different measurements. Circles represent the transition temperatures obtained from the calorimetry measurement. Diamond shows the transition temperature obtained from resistivity in a diamond cell. Squares show results from previous resistivity measurements (Refs. 4 and 5). Lines are guides for the eyes.

The curve of the magnetic-ordering temperature T_M with pressure is nearly linear above 8.5 GPa, though slightly steeper below 10 GPa. The dashed line indicates the anomalies found at lower pressures where no well-defined transition was seen. In the previous studies,^{4,5} where the magnetic-ordering temperature was determined from resistivity measurements, at pressures above 10 GPa, a clear anomaly was seen in the resistivity, however at lower pressure the signature was weak and could only be extracted by taking the derivative. Below 8.5 GPa no sign of a magnetic transition could be seen. The transitions found in our specific-heat measurements are in general sharper and the determination of T_M is less ambiguous to within about 0.15 K. We cannot say whether this is mainly due to the different type of measurement, more hydrostatic conditions, or improved sample quality. Probably all three factors play a role. Our high-pressure data is in good agreement with the data of Alami-Yadri *et al.*⁴ However despite this we are not able to accurately follow the transition below 8.1 GPa and about 1.5 K. The fact that magnetic order seems to appear at around 1.5 K might point to a first-order pressure-induced transition as previously suggested by Winkelmann *et al.*,⁵ backed up by the apparent coexistence of a magnetic and a nonmagnetic component in the Mössbauer spectra.

In the previous part all specific-heat curves were normalized in the high-temperature part in order to compare curves obtained in different conditions. Indeed this type of measurement is not quantitative as it is impossible to determine the power that is absorbed by the sample. However, when using the *in situ* pressure-tuning device we could change the pressure while all other factors remain constant. We can therefore semiquantitatively compare some curves at different pres-

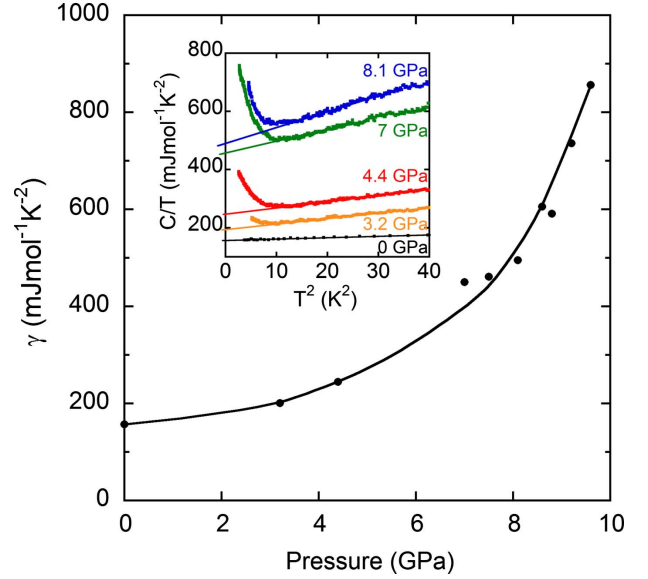


FIG. 4. (Color online) Estimated pressure dependence of the γ coefficient obtained from the specific heat in the temperature range above about 3 K (calculated as explained in the text). The inset shows the linear dependence of C/T versus T^2 from which γ was estimated.

ures. Selected curves are shown in the inset of Fig. 4 where we clearly see a strong increase in the specific heat with pressure, as well as the appearance of an upturn at low temperature. We estimated the electronic contribution to the specific heat by a fit $C/T = \gamma + \beta T^2$ for temperatures between the upturn and 10 K. This pressure dependence (approximated by a second degree polynomial) was then extrapolated to the known value at ambient pressure in order to obtain the pres-

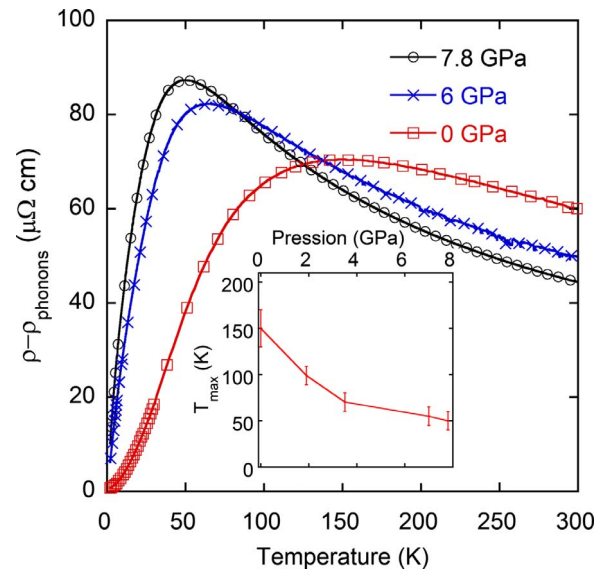


FIG. 5. (Color online) Selected electrical resistivity curves of YbCu_2Si_2 under pressure in a modified Bridgman cell showing the evolution of the maximum in the resistivity. The phonon contribution has been subtracted. Inset: pressure dependence of the maximum resistivity temperature T_{\max} . Error bars represents magnitude of T_{\max} differences from one pressure cell to the other.

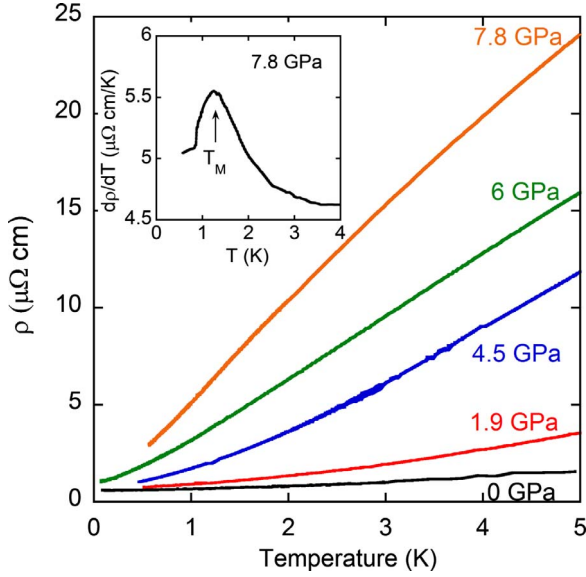


FIG. 6. (Color online) Resistivity of YbCu_2Si_2 under pressure at low temperature. The 7.8 and 6.0 GPa measurements were performed in a modified Bridgman cell. The 1.9 and 4.5 GPa measurements were performed in a diamond-anvil cell down to 500 mK. The inset shows the temperature derivative of the resistivity at 7.8 GPa showing the maximum which we attribute to the magnetic transition.

sure dependence of γ shown in Fig. 4. We find that γ attains a value of approximately 850 mJ/mol K² corresponding to an increase by more than a factor 5 from ambient pressure. We point out that this value is obtained from the temperature range approximately 3–10 K whereas at very low temperatures C/T certainly reaches much higher values. This point will be discussed further on.

Resistivity measurements were performed in the diamond-anvil cell up to 7.8 GPa, in the ⁴He cryostat with the *in situ* pressure-tuning device,⁸ and at several fixed pressures down to 500 mK in the ³He cryostat. Measurements were also carried out in the modified Bridgman cell down to 60 mK in the dilution refrigerator. Figure 5 shows the temperature dependence of the resistivity after subtraction of the phonon contribution taking the nonmagnetic system LuCu_2Si_2 (Ref. 15). We observe a strong decrease in the resistivity maximum temperature T_{max} from around 150 K at ambient pressure to around 50 K for the highest pressures reached. Differences in the T_{max} already noticed at ambient pressure from one sample to the other are confirmed under pressure and we attribute this to slightly different orientations of the sample. The decrease in T_{max} is much stronger at lower pressures up to around 4 GPa. As the maximum is shifted to lower temperatures with pressure, it also becomes more pronounced. The changes in the resistivity curves with pressure at low temperature are shown in Fig. 6. The highest pressure reached was about 7.8 GPa though there is some uncertainty on the value of the pressure at this point as there was a problem with the lead manometer. The pressure was estimated from the high-temperature behavior of the sample in comparison to our other results. At this pressure, a weak anomaly around 1.3 K is seen which we attribute to the mag-

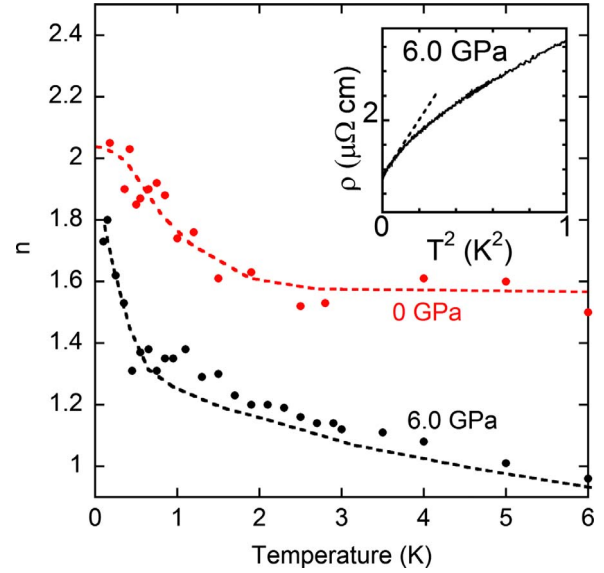


FIG. 7. (Color online) Temperature dependence of the exponent n for $p=0$ and $p=6$ GPa (close to the critical point) obtained by a fit to the form $\rho - \rho_0 = AT^n$ with a sliding window (see text). At 6 GPa a T^2 dependence is never completely reached, although a T^2 law appears to fit the data up to about 300 mK (inset).

netic transition. In the inset we show the derivative which has a small but clear maximum. Using the criterion of the maximum of $d\rho/dT$ we find that the transition temperature agrees with the higher pressure data obtained from the calorimetry measurements and the previous resistivity study.⁴ As pressure increases the temperature range over which a T^2 Fermi-liquid behavior describes the data becomes smaller. While at ambient pressure a T^2 behavior was found up to 0.9 K, at 6 GPa this fit is a good description only up to 350 mK. To better characterize the power laws we show in Fig. 7 for two pressures (0 and 6 GPa) the temperature dependence of the exponent n of a sliding window (typically 100 mK) fit to the form $\rho - \rho_0 = A_n T^n$, where ρ_0 is fixed and obtained from the fit at the lowest temperature (0.06–0.15 K). This confirms that whereas at ambient pressure a T^2 behavior is reached approximately below 1 K, at 6 GPa the T^2 behavior, although approached, is never completely obtained and that n decreases very rapidly with temperature. At higher temperature we have a $T^{1.5}$ behavior at $p=0$ and at $p=6$ GPa the temperature dependence approaches a linear behavior. Although at high pressure a T^2 dependence is not completely reached, it is nevertheless useful to look at the pressure dependence of A , the coefficient if we force a fit to the form $\rho - \rho_0 = AT^2$ at low temperature. This is illustrated by the linear dependence represented by the dashed line in the inset where the resistivity versus T^2 at 6 GPa is shown down to 60 mK. In the measurements that were performed in a diamond-anvil cell and the ³He cryostat, the lowest temperature was 0.5 K. To follow the A and ρ_0 dependence from these results, we forced a T^2 fit for data with $0.5 < T < 1$ K. This was an acceptable approximation for pressures lower than 4 GPa but gives underestimated A values and overestimated ρ_0 values at higher pressures. In Fig. 8 the results from the T^2 fits are shown, together with the previously reported values.⁴ The depen-

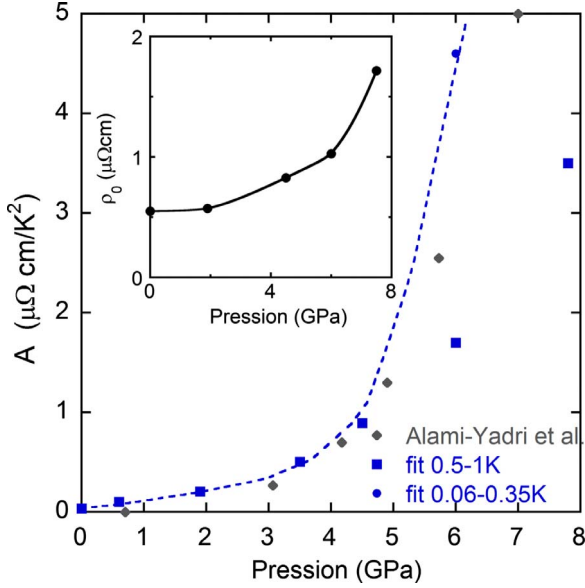


FIG. 8. (Color online) A and ρ_0 from a T^2 fit. Different symbols correspond to different temperature ranges for the fit: Up to about 4 GPa the fit in the temperature range 0.5–1 K (full squares) gives a good value but at higher pressure the value depends strongly on the temperature range of the fit and a fit over the lowest range 0.06–0.35 K (full circles) gives a much higher value. Diamonds represent the data from Alami-Yadri *et al.* (Ref. 4). The dashed line is a guide to the eyes indicating what we believe to be the true low-temperature behavior. Inset shows the variation in ρ_0 with pressure for the low measurement in the diamond and modified Bridgman cells.

dence of the value of A on the temperature range of the fit is clear. We observe that at 6 GPa a fit in the 0.5–1 K temperature range compared to a low-temperature fit (60–350 mK) gives a ρ_0 value two times higher and an A value approximately three times lower. A T^2 fit between 60 and 350 mK for 6 GPa gives $\rho_0 = 1.07 \mu\Omega \cdot \text{cm}$ and $A = 4.6 \mu\Omega \cdot \text{cm}/\text{K}^2$. From the ambient pressure value, this represents an increase of a factor 58 for A and less than 2 for ρ_0 . This very small increase in ρ_0 is in good agreement with the one previously found.⁴

In most cerium-based heavy fermion systems, the Kadowaki Woods¹⁶ ratio A/γ^2 , assumes a common value $R_{KW} = 10^{-5} \mu\Omega \cdot \text{cm} \cdot \text{mol}^2 \cdot \text{K}^2 \cdot \text{mJ}^{-2}$. However in many intermediate-valence ytterbium-based systems, the Kondo temperature T_K can be of the same order or larger than the crystal-field temperature T_{CEF} leading to a reduced value of the ratio due to the degeneracy of the ground state.^{17,18} For example a ratio A/γ^2 of about 0.07 R_{KW} has been found in YbNi_2Ge_2 (Ref. 19) and YbInCu_4 (Ref. 20) and this has been shown to be compatible with a full orbital degeneracy.¹⁷ The case of YbCu_2Si_2 is less extreme and we find $A/\gamma^2 = 0.4 R_{KW}$, a value similar to that found in YbIr_2Si_2 (Ref. 21) implying an intermediate degeneracy (the formula¹⁸ would give a value of 3). Applying pressure drives ytterbium closer to its Yb^{3+} state, decreases T_K and by reducing the degeneracy can lead to an increase in the ratio. One difficulty in evaluating the Kadowaki Woods ratio under pressure is estimating the value of γ which can change strongly especially

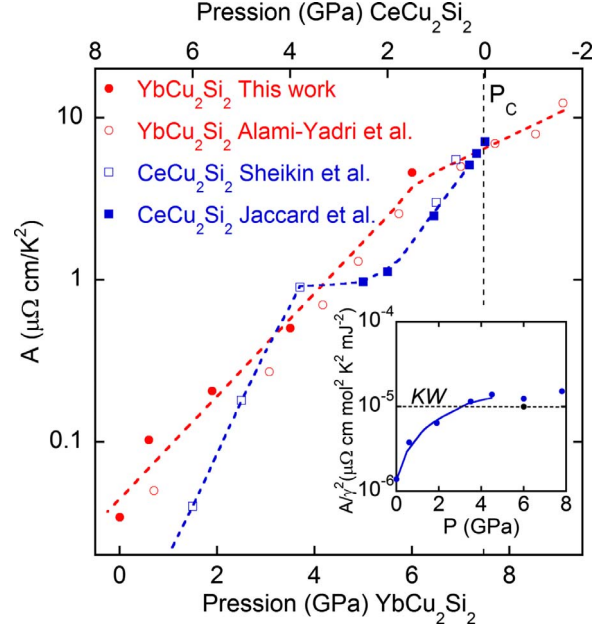


FIG. 9. (Color online) Comparison of the evolution of the T^2 term of the resistivity with pressure in YbCu_2Si_2 and CeCu_2Si_2 (Refs. 24 and 25). To take into account the opposite effect of pressure on cerium and ytterbium systems, the pressure scale for CeCu_2Si_2 (top) has been inverted. The scale has also been shifted so that the critical pressures coincide. Lines are guides for the eye. Inset: Evolution of the ratio A/γ^2 with pressure. Values for g are determined from the ac calorimetry measurement under pressure for $T > 3$ K. A is determined from a fit of the resistivity in the temperature range 0.5–1 K. The solid line shows the pressure range where this fit gives a correct value for A . The black square shows the value if the very low-temperature values of A and C/T are taken. (see text for the discussion).

near a critical point. Most studies rely on the assumption that the maximum in the resistivity can be associated with T_K , which in turn is assimilated to γ^{-1} . In the present study we have in addition an approximate but direct estimation of the evolution of γ with pressure. In fact both approaches are compatible as we find in the pressure range up to 8 GPa γ increases by about a factor 4 whereas T_{max} decreases by a similar factor. In the inset of Fig. 9 we show the evolution of the Kadowaki Woods ratio as a function of pressure taking the value for γ obtained from the calorimetry measurements and the values for A found from the fit in the temperature range 0.5–1 K. In the pressure range where this gives a reasonable value for A (up to 4 GPa), we find A/γ^2 saturates at a value close to the universal value. On the other hand if the very low-temperature data is taken, we find A/γ^2 of about 3.4 R_{KW} . At 6 GPa. However we should point out that the value for γ was determined by extrapolating the high temperature ($T > 3$ K) of C/T and that at the very low temperatures C/T does not follow Fermi-liquid behavior but is strongly increasing with decreasing temperature. In these conditions the validity of the Kadowaki Woods analysis using the high-temperature extrapolation of γ is questionable. If at 6 GPa we take the estimated value of C/T at low temperature (700 mJ/mol K²) and the low-temperature value for A (4.5 $\mu\Omega \cdot \text{cm}/\text{K}^2$) we find a ratio of almost exactly

$10^{-5} \mu\Omega \text{ cm mol}^2 \text{ K}^2 \text{ mJ}^{-2}$. The situation in this pressure range (6–8 GPa) is quite similar to the case of YbRh_2Si_2 at ambient pressure where at low temperature a value of $A = 20 \mu\Omega \text{ cm/K}^2$ is reported²² and C/T is not constant but reaches about 1500 mJ/mol K^2 at the lowest temperature measured²³ which would give $A/\gamma^2 = R_{\text{KW}}$. This is compatible with Yb reaching its 3+ state at high pressure with a degeneracy of 2.

It is interesting to compare the pressure dependence of A in YbCu_2Si_2 , with that of its cerium counterpart CeCu_2Si_2 .^{24,25} In Fig. 9 we have shown this where the pressure scale has been inverted for CeCu_2Si_2 , to take into account the opposite effect of pressure on cerium systems compared to ytterbium and shifted so that the critical pressures for both compounds coincide. The overall behaviors are quite similar with an increase of more than 2 orders magnitude of A as the critical pressure is approached from the paramagnetic phase over a pressure range of 8 GPa. At least three factors play a role in this increase: The decrease in T_K is naturally accompanied by an increase in the effective mass. Simultaneously as T_K becomes smaller than T_{CEF} the effective degeneracy decreases as described in the previous paragraph. Third as magnetic order is approached, spin fluctuations introduce another contribution. Looking closer at the increase in A on approaching the critical pressure in CeCu_2Si_2 , this occurs in two steps. The first step ($4 < p < 6$ GPa) probably corresponds to a sharp change in the cerium valence²⁴ whereas the second step ($0 < p < 2$ GPa) can be attributed to the contribution of spin fluctuations on approaching the magnetic critical point. In contrast for YbCu_2Si_2 , A increases more smoothly. As stated above, several factors enter into the variation in A and we cannot make any definite statement on the Yb valence but we expect that for ytterbium the valence can change considerably more than for cerium and that here this is occurring over a much larger pressure range. Hence the effect of the transition toward the Kondo lattice heavy fermion state and the effect of spin fluctuations are mixed. Furthermore, whereas the effect of spin fluctuations should produce a pronounced maximum of A at the magnetic critical pressure, from the previous studies it was found that A increases continuously with pressure even above the critical pressure and reaches a value of about $20 \mu\Omega \text{ cm/K}^2$ at 10 GPa.^{3–5} Although in our present study, resistivity measurements were not performed at pressures much higher than the critical pressure, we do not find a maximum. This implies that the contribution of spin fluctuations to the resistivity is weak compared to the combined

effects of the valence change and the pressure dependence of the Kondo temperature. This difference between the Ce and Yb system is probably not generic as in Ce systems a variety of behaviors is found: in several systems the valence transition probably coincides with the magnetic critical point²⁶ and in $\text{CeCu}_{6-x}\text{Au}_x$ the increase in A is quite continuous.¹⁴

Finally, while superconductivity at a quantum critical point in cerium-based compounds is becoming the rule rather than an exception, there is still only one example in an ytterbium system.² In this study no signs of superconductivity were found when the resistivity was measured down to 60 mK at 6 GPa. A systematic search for superconductivity is planned for future experiments.

IV. CONCLUSION

We have grown and characterized high quality single crystals of YbCu_2Si_2 . At ambient pressure extrapolated residual resistivity ratios of up to $\text{RRR}_{0-300 \text{ K}} = 300$ are found corresponding to a residual resistivity of about $0.2 \mu\Omega \text{ cm}$. We have also determined the anisotropy of the temperature dependence of the resistivity and shown that this can account for sample-dependent differences of the resistivity. We have performed resistivity and ac calorimetry measurements under pressure in diamond and Bridgman anvil pressure cells with liquid pressure-transmitting media. We have precisely determined the (p, T) phase diagram using calorimetry measurements and we confirm the previously reported transition to a magnetically ordered ground state with pressure. The transitions are well defined above 8.8 GPa but still we are unable to obtain clear transitions below 1.6 K and 8.1 GPa and this probably is further evidence for a first-order transition. We have analyzed the low-temperature resistivity and specific-heat behaviors. At ambient pressure YbCu_2Si_2 shows a moderately reduced Kadowaki Woods ratio similar to many other Yb systems due to degeneracy of the Yb ground state. This ratio is found to increase with applying pressure. We discuss the difficulties in evaluating the Kadowaki Woods ratio under pressure and show that with the combination of transport and calorimetry measurements we can have a more direct evaluation. We compare the results to the universal Kadowaki Woods ratio to other ytterbium-based strongly correlated systems, and to the cerium-based counterpart CeCu_2Si_2 . We suggest that contrary to the case of CeCu_2Si_2 , in YbCu_2Si_2 the valence change in the rare earth is larger and also occurs over a much wider pressure range. At the critical pressure spin-fluctuation effects are probably dominated by the valence change and the pressure dependence of the Kondo temperature.

¹J. Flouquet, in *Progress in Low Temperature Physics*, edited by W. Halperin (Elsevier, Amsterdam, 2005), Vol. XV.

²S. Nakatsuji, K. Kuga, Y. Machida, T. Tayama, T. Sakakibara, Y. Karaki, H. Ishimoto, S. Yonezawa, Y. Maeno, E. Pearson, G. G. Lonzarich, L. Balicas, H. Lee, and Z. Fisk, *Nat. Phys.* **4**, 603 (2008).

³K. Alami-Yadri and D. Jaccard, *Solid State Commun.* **100**, 385

(1996).

⁴K. Alami-Yadri, H. Wilhelm, and D. Jaccard, *Eur. Phys. J. B* **6**, 5 (1998).

⁵H. Winkelmann, M. M. Abd-Elmeguid, H. Micklitz, J. P. Sanchez, P. Vulliet, K. Alami-Yadri, and D. Jaccard, *Phys. Rev. B* **60**, 3324 (1999).

⁶E. Colombier and D. Braithwaite, *Rev. Sci. Instrum.* **78**, 093903

- (2007).
- ⁷A. Demuer, C. Marcenat, J. Thomasson, R. Calemczuk, B. Salce, P. Lejay, D. Braithwaite, and J. Flouquet, *J. Low Temp. Phys.* **120**, 245 (2000).
 - ⁸B. Salce, J. Thomasson, A. Demuer, J. J. Blanchard, J. M. Martinod, L. Devoille, and A. Guillaume, *Rev. Sci. Instrum.* **71**, 2461 (2000).
 - ⁹N. Tsujii, H. Kitazawa, T. Aoyagi, T. Kimura, and G. Kido, *J. Magn. Magn. Mater.* **310**, 349 (2007).
 - ¹⁰T. Shimizu, H. Yasuoka, Z. Fisk, and J. L. Smith, *J. Phys. Soc. Jpn.* **56**, 4113 (1987).
 - ¹¹B. C. Sales and R. Viswanathan, *J. Low Temp. Phys.* **23**, 449 (1976).
 - ¹²H. C. Montgomery, *J. Appl. Phys.* **42**, 2971 (1971).
 - ¹³T. Moriya and K. Ueda, *Adv. Phys.* **49**, 555 (2000).
 - ¹⁴HV. Löhneysen, *J. Phys.: Condens. Matter* **8**, 9689 (1996).
 - ¹⁵D. Wohlleben and B. Wittershagen, *Adv. Phys.* **34**, 403 (1985).
 - ¹⁶K. Kadowaki and S. B. Woods, *Solid State Commun.* **58**, 507 (1986).
 - ¹⁷H. Kontani, *J. Phys. Soc. Jpn.* **73**, 515 (2004).
 - ¹⁸N. Tsujii, H. Kontani, and K. Yoshimura, *Physica B* **378-380**, 730 (2006).
 - ¹⁹G. Knebel, D. Braithwaite, G. Lapertot, P. C. Canfield, and J. Flouquet, *J. Phys.: Condens. Matter* **13**, 10935 (2001).
 - ²⁰T. Park, V. A. Sidorov, J. L. Sarrao, and J. D. Thompson, *Phys. Rev. Lett.* **96**, 046405 (2006).
 - ²¹H. Q. Yuan, M. Nicklas, Z. Hossain, C. Geibel, and F. Steglich, *Phys. Rev. B* **74**, 212403 (2006).
 - ²²G. Knebel, R. Boursier, E. Hassinger, G. Lapertot, P. G. Niklowitz, A. Pourret, B. Salce, J. P. Sanchez, I. Sheikin, P. Bonville, H. Harima, and J. Flouquet, *J. Phys. Soc. Jpn.* **75**, 114709 (2006).
 - ²³O. Trovarelli, C. Geibel, and F. Steglich, *Physica B* **284-288**, 1507 (2000).
 - ²⁴D. Jaccard, H. Wilhelm, K. Alami-Yadri, and E. Vargoz, *Physica B* **259-261**, 1 (1999).
 - ²⁵I. Sheikin, D. Braithwaite, J.-P. Brison, W. Assmus, and J. Flouquet, *J. Low Temp. Phys.* **118**, 113 (2000).
 - ²⁶A. T. Holmes, D. Jaccard, and K. Miyake, *J. Phys. Soc. Jpn.* **76**, 051002 (2007).